

A Software System for Laser Design and Analysis

P. L. Cross
N. P. Barnes
E. D. Filer*

NASA Langley Research Center
Hampton, Virginia 23665-5225

ABSTRACT

The unique demands of space-based lasers for atmospheric remote sensing require the development of high efficiency, narrow line width lasers throughout the .280 μm to 10.0 μm region.^{1,2} The combination of laser performance requirements, large number of candidate laser materials, and complex mathematical models necessitates the development of an integrated, computerized software system consisting of a database, laser models, and a user-friendly software interface. Such a three part software system for laser design is under development. The three parts include: a database of laser, optical, and nonlinear materials; laser component, amplifier, resonator, and oscillator models; and a menu-driven interface.

1. INTRODUCTION

Atmospheric remote sensing is one of the roles and missions of NASA Langley Research Center. Atmospheric remote sensors provide data pertaining to atmospheric chemistry and dynamics, meteorology, altimetry, and wind shear. The cycles of the oxides of nitrogen, chlorine, and hydrogen are investigated as part of atmospheric chemistry and dynamics. Water vapor, temperature, pressure, and winds are measured meteorological parameters. Range-resolved vertical profiles of the atmospheric constituents are preferred over total burden measurements. Laser-based Light Detection And Ranging (LIDAR) instruments measure range-resolved vertical profiles of atmospheric constituents. To design lasers for LIDAR systems and to assess their performance, a laser material database and a laser modeling software system has been developed.

2. OVERVIEW

A schematic of the software system for laser design is shown in Figure 1. The software system contains three basic sections: database LASERS³, the laser models, and the interface software. Database LASERS contains the physical parameters of laser, optical, and nonlinear materials which are required by laser models. The laser models include efficiency calculations, electro-optical component models, laser resonator, amplifier, and oscillator models, and miscellaneous models. The interface software provides a user-friendly interface between the user and his personal data files, the database, and the laser models.

The user-friendly, interactive database contains 2 parts: spectra and tabulated data. Three types of spectra can be found in database LASERS:

Planning Research Corporation, Hampton, Virginia

laser materials absorption spectra, laser materials emission spectra, and laser diode emission spectra. Approximately 25 tables containing 190 unique columns of data compromise the tabulated data. The tabulated data consists of tables of thermal, mechanical, optical, and crystalline properties of laser, optical, and nonlinear materials. The tabulated section of the data-base runs under the commercially available data-base management software, R:BASE for DOS. Data is retrieved from the tabulated section of the data-base by entering the appropriate Standard Query Language (SQL) command or by executing preprogrammed macros. Macros are programs written in the R:BASE database language and are used to retrieve data from the database, to load data into the database, or to maintain the data base.

The laser modeling software which has been completed to date is listed in Table 1. Our initial efforts for developing laser software targeted data acquisition, reduction, and analysis software, electro-optical component models, and efficiency calculations. Data acquisition, reduction, and analysis software was created to support laser and spectroscopic laboratories. Electro-optical component models were required to design and analyze narrow line width lasers with the desired laser center frequency. To guide the selection of relatively efficient laser materials for more detailed spectroscopic study, models which calculated the efficiency of various laser processes were developed. Studies using those models were conducted to determine the most efficient laser material under various conditions. Current efforts are directed toward development of laser amplifier, resonator, and oscillator models.

The interface software allows a user to easily execute the laser models and to query the database. Figure 2 shows a schematic of the directory structure for the laser modeling software system. As indicated in the figure, the major parts of the directory structure are the database, the laser models, the user's data files, and the interface software. The user's data files contain data for a specific laser model. A user's data file may contain either input data or output data. For example, a user's file may contain the calculated absorption efficiency for a specific laser material and geometry. At run time, physical parameters of materials data are available from the database. The menu-driven software interface enables a user to get on-line help, to make database queries, to execute database macros, to access software utilities, and to execute laser models. By using the software interface, the user is not required to know the directory structure, program names, or macro names. As with all menu-driven interfaces, the user simply picks a menu option.

The software design and development philosophy emphasized flexibility, ease of use, and development and maintenance costs, as well as performance. To minimize development costs, commercially available and public domain software was used whenever possible. Commercially available software includes a database manager, graphics subroutine library, menu maker, and various compilers, assemblers, and interpreters. CMLIB, a public domain math library available from NIST, was also used. Approximately 10 MByte of disc space is currently required to store the complete software system. Roughly 5 Mbytes can be allocated to the commercially available software and 3 Mbytes to the database.

3. DISCUSSION OF THE SOFTWARE

3.1 Laser Models

As indicated in Figure 1, the laser models can be divided into four categories: efficiency calculations, electro-optical component models, laser amplifier, resonator, and oscillator models, and miscellaneous models.

The absorption efficiency is an extremely important component of the laser efficiency. Three models for calculating the laser absorption efficiency exist. These models are identical except for the pump source. The three models correspond to a flashlamp pumped laser modelled using a blackbody source⁴, a laser diode pumped laser (modelled as a Gaussian intensity profile source⁵, and a user-supplied spectrum pumped laser. All three models require the user to select a rod or slab geometry, the rod radius or slab thickness, as appropriate, the active-atom concentration, and one of four angular distribution functions. The four angular distribution functions are uniform, Lambertian, symmetric Gaussian, and asymmetric Gaussian. The range of Gaussian center wavelengths and full width half-maximums or the range of blackbody temperatures, as appropriate, and the number of sources are also required by the models. A related model for only the rod geometry allows the user to calculate the radial distribution of absorbed energy. A laser oscillator model with 2 degrees of freedom, radial distance and time, is currently under development. The output of the radial distribution of absorbed energy model is used as an input to this laser oscillator model. All four models utilize absorption spectra from database LASERS.

Figures 3 and 4 show the absorption efficiency calculated using the laser diode pumped laser absorption efficiency model. In both figures, a Lambertian angular distribution function was selected, a rod geometry was used, and the material was Nd:YAG. Figure 3 shows the absorption efficiency as a function of laser diode center wavelength for two values of laser diode full-width half-maximum (FWHM). For the curve with the most structure, the laser diode FWHM was .001 micrometers. The other curve had a FWHM of .004 micrometers. In Figure 3, the rod radius times concentration product was .02 mm. This corresponds to a rod of 2.0 mm radius doped with 1 percent Nd. As expected, the wavelength of maximum absorption efficiency for the narrow FWHM diode lies at the peak of the absorption spectrum, .808 micrometers. For the broader FWHM, the wavelength of maximum absorption efficiency is slightly smaller. Since laser diode center wavelength depends on temperature, plots such as Figure 3 can be used to determine the effect of laser diode temperature changes on the laser efficiency. The absorption efficiency for the smaller FWHM case changes much more rapidly and to a greater extent than for the larger FWHM. Hence, laser diode pumped lasers with small full-width half-maximums are more sensitive to temperature changes than laser diode pumped lasers with larger full-width half-maximums. To maintain a high efficiency, laser diode pumped, Nd:YAG lasers with small laser diode full-width half-maximums should be temperature controlled. Figure 4 shows the absorption efficiency as a function of the product of the rod radius and concentration for two values of laser diode FWHM. In this figure, the full-width half-maximums are .002 micrometers and .005 micrometers. The laser diode center wavelength was fixed at .808 micrometers. The absorption efficiency was calculated and a cubic spline was fit through the points to yield Figure 4. By choosing a rod size, plots of this form can be used to determine the sensitivity

of the absorption efficiency to uncertainties in the dopant concentration. Alternately, by fixing the dopant concentration they can be used to determine the sensitivity of the absorption efficiency to rod size. Obviously, the sensitivity of the absorption efficiency to the laser diode FWHM can also be determined. Plots of the form given in Figures 3 and 4 can be generated for any material whose absorption spectra is in database LASERS.

Figures 5 and 6 show the absorption efficiency calculated using the blackbody pumped laser absorption efficiency model. Both figures are for a Lambertian angular distribution function and a rod geometry. Figure 5 uses a Nd:YAG⁶ spectrum. Figure 6 uses spectra from the database for Nd:YVO₄^{7,8}, Nd:YLF⁹, Nd:YAG, Nd:Cr:GSGG¹⁰, Nd:Glass¹¹, and Nd:BEL¹². Figure 5 shows the absorption efficiency as a function of blackbody temperature for two values of rod radius times concentration product. Figures of this form allow the user to determine the optimum blackbody temperature, the sensitivity of absorption efficiency to changes in the blackbody temperature, and the effects of rod size and/or dopant concentration changes. Figure 6 shows the absorption efficiency as a function of rod radius times concentration for a 9500 K blackbody for 6 Nd doped laser materials. Figures of this form can be used to determine the best absorber for a selected rod size and dopant concentration. They can also be used to determine the sensitivity of the absorption efficiency to changes in the rod size or dopant concentration for a selected laser material. As with the laser diode pumped model, these calculations can be performed on any material whose absorption spectrum is in database LASERS.

Sensitizer transfer rates can be calculated using the Dexter theory of energy transfer between ions¹³. Computation of the integrals involved in Dexter's theory of atom-to-atom energy transfer required an active atom absorption spectra and a sensitizer emission spectra. In general, tabulated energy levels of laser crystalline materials are more readily available than digitized absorption and emission spectra. Hence, a sensitizer transfer rate model using tabulated energy levels is under development. This model will be used to select the best candidate materials for sensitized lasers. After using this model to narrow the list of potential laser materials, spectroscopic samples and laser rods will be acquired for further comparative studies.

The birefringent filter¹⁴ and etalon models are used to determine the effects of these components on a laser's spectral properties. These two models were designed to help the laser designer assess the performance of the components in a specific application. These models can be used to determine the effects of thermal instability, mechanical misalignment, and manufacturing errors on the component's performance. In other words, both models were written broadly enough to allow the laser designer to determine thickness tolerances, alignment criteria, and temperature sensitivity. The etalon model can assess the effects of wedges, surface roughness, and temperature in addition to the mirror reflectivity and etalon tilt. The birefringent filter model has three angular degrees of freedom, the azimuthal, polar, and rotation angles. Up to 12 plates may be specified for the birefringent filter. The input state of polarization and the desired output state of polarization are specified at run time.

Figures 7 and 8 demonstrate some of the capabilities of the birefringent filter model. In both figures, p-plane light was incident into the filter

and the p-plane transmission of the filter was calculated. The filter was constructed of 4 quartz plates with thickness ratio 2:3:6:18 and base thickness of 0.25 mm. Details of the filter are given in reference 14. Figure 7 shows the p-plane transmission as a function of rotation angle at .785 micrometers. Figures such as Figure 7 could be used to help align a birefringent filter. Figure 8 shows the p-plane transmission as a function of wavelength. Figure 8 can be used to help determine the line narrowing and light blocking capabilities of a birefringent filter.

A laser amplifier model accounts for both nonuniform pump energy deposition and non-negligible loss at the laser wavelengths. Nonuniform deposition of the pump energy occurs commonly with laser pumped laser amplifiers, such as Ti:Al₂O₃. Both radial and longitudinal nonuniformities have been successfully modelled although azimuthal symmetry has been assumed. Beams with both Gaussian and circular beam profiles have been modelled as extracting input beams. While the inclusion of loss in a laser amplifier is straightforward, its inclusion prevents the solution of the Frantz Nodvek equations in closed form. Results from the laser amplifier model have shown that even relatively by small losses at the laser wavelength can significantly affect the efficiency of the laser amplifier. Predictions of the laser amplifier model have been verified by comparing them with well-characterized experiments performed with a laser pumped Ti:Al₂O₃ amplifier.¹⁵

The laser resonator model is patterned after the Gaussian beam propagation technique outlined in Kogelnik and Li.¹⁶ This model calculates the beam radius on the input surface of each element. Using this information and the laser output power, the power density on each element can be calculated. For lasers operating near the damage threshold, the power density on each laser element is very important. The model allows the user to configure the laser as either a ring or a Fabry Perot resonator. Up to 50 elements either internal to or external to the cavity are permitted. Each element may be defined as a lens or mirror, parallel plate, dummy surface, or a Gradient Index (GRIN) lens. Gradient index lenses can be used to model the effects of a temperature distribution across the laser rod.

Figure 9 shows an example of the laser resonator model. A three element laser configured as a Fabry-Perot resonator was modelled. The first element was a mirror with a focal length of 2.5 m, the second element was a lens with focal length 3.0 m located .5 meters from the first element, and the third element was a flat mirror located .7 m from the second element. The beam radius as a function of position was calculated at each element and at many dummy surfaces between the elements. A cubic spline was fit through the calculated points. A plot of this form, along with some additional information could be used to calculate the power density anywhere inside the laser cavity.

The rubidium cell transmission model¹⁷ was used to design an experiment for measuring amplified spontaneous emission (ASE) and to interpret the results of the experiment. Briefly, the Rb cell, which absorbs energy at approximately .780 μm , blocks the central portion of the laser pulse and transmits only in the wings of the laser pulse. For lasers with center wavelength corresponding to the Rb center wavelength, the residual transmitted energy corresponds to the ASE.

The temperature distribution in the laser rod model¹⁸ calculates the thermal distribution inside a laser rod for a variety of rod geometries, optical pumping configurations, cooling techniques, and pulse-repetition frequencies.

3.2 Interface Software

The obvious advantages of the menu-driven interface were discussed in the introduction. A key property of the software system is the extensive use of file headers. Roughly 30 types of data files are associated with the laser modeling software system. File headers allow a user to identify a file's contents long after the file has been created. Headers can also be used to trace the path which data takes through the software system. Unique features of the file headers enable computer software to identify the source of a data file. The software is sophisticated enough to lock itself out of inappropriate data files.

Most data files associated with the software system for laser design have a header. Table 2 shows a header from an absorption spectra. The header is terminated by an End-Of-Header (EOH) record. The record immediately following the EOH record contains the number of data points in the data section of the file. Finally, the first few lines of the spectrum are listed. Absorption spectra contain only one column of data, the absorption for unity concentration. In the software, the wavelength for each record is calculated from the minimum wavelength and resolution given in the header. The header contains three types of data: information common to all file headers, information common to all absorption spectra files, and comments. Header information common to all file headers is listed in Table 3. Header information unique to the absorption spectra is listed in Table 4. The records immediately preceding the EOH record contain comments unique to this spectrum. These lines were inserted by the operator during file conversion and transfer.

The first field on the header is the program code which is unique to each type of data file. For example, the birefringent filter model requires two input data files and can generate up to three output data files. One type of input data file contains filter component data: the other contains the filter's material properties. The filter component data file includes design data, such as azimuthal angle, polar angle, rotation angle, and thickness for each plate in the filter. The materials data file contains the material's properties, such as Sellmeier coefficients and the thermal expansion coefficients. The three possible output files are the modified filter component data file, the transmission versus wavelength, and the Jones' matrix vs. wavelength. A Jones matrix versus wavelength output is useful for determining the eigen polarizations. The modified filter component data file may be used as an input file for subsequent runs. Since four unique types of files are associated with the birefringent filter model, four unique program codes exist for this model. A program code library contains a list of acceptable program codes for input data files for each program.

The file headers with their program codes and the program code library together serve several purposes. First, the user can easily identify the software with which a data file is associated. If the user has only a few files and the files did not contain the headers, he could easily forget the meaning of the numbers on any particular file. Second, each program accesses files appropriate only to itself. For example, if the user inadvertently accesses a file containing etalon data when executing the birefringent filter model, the program prints an error message to the screen and requests another data file name. Third, the interface software can identify the module which generated a specific file. Software can be created which allows the user to list file names for only one type

of file. For example, the user may want to know the names of all files containing the absorption efficiency of a laser pumped laser. Fourth, since program codes are unique to each type of data file, the format and units of the data section of the file are immediately known. A single plot program is being created to plot data for any software module. By exploiting the potential of the program codes, the plot program will include default labels and formats for all software modules in the system.

4.0 CONCLUSIONS

The structure of a software system for laser design is essentially in place. To date, 12 major laser models have been completed. The models include: efficiency calculations, electro-optical component models, laser amplifiers and resonators, and miscellaneous models. Plans call for continued development of all three components of the software system: data will be added to the database on an as-needed basis; laser models and data base macros will continue to be developed, and plot and directory maintenance capabilities will be added to the interface software. Plans also call for upgrading the computer hardware and software. The new computer system will support a multi-user, multi-task operating system.

Three of the models discussed in this paper are available through COSMIC, NASA's clearing house for software. They are LAR-13945 "Birefringent Filter Model", LAR-14055 "Etalon Model", and LAR-14080 "Gaussian Beam - Laser Resonator Model". To acquire a copy, contact COSMIC, University of Georgia, 382 East Broad Street, Athens, Georgia, 30602. The temperature distribution inside the laser rod model has been submitted to COSMIC but has not yet worked its way through the system.

5.0 REFERENCES

- 1) M. M. Sokolowski, F. Allario, and R. R. Nelms, "Technology for Active Laser Remote Sensing from Space", 37th IAF Congress on Space: New Opportunities for All People, Innsbruck, Austria, 1986.
- 2) F. Allario and M. M. Sokolowski, "NASA's Technology Program for Active Remote Sensing," SPIE OE Lase '87, 1987.
- 3) P. L. Cross, E. D. Filer, N. P. Barnes, M. W. Skolaut, Jr., "A Database for Solid State Laser, Optical, and Nonlinear Materials", SPIE OE Lase '90, Los Angeles, California, 1990.
- 4) P. L. Cross, N. P. Barnes, M. W. Skolaut, Jr., and M. E. Storm, "Blackbody Absorption Efficiencies for Six Lamp Pumped Nd Laser Materials", to be published in February 1990, issue of Applied Optics.
- 5) N. P. Barnes, M. E. Storm, P. L. Cross, and M. W. Skolaut, Jr., "Efficiency of Nd Laser Materials with Laser Diode Pumping", accepted by J. Quantum Electronics.
- 6) J. E. Geusic, H. M. Macros, and L. G. Van Ulitert, "Laser oscillations in Nd-doped yttrium aluminum, yttrium gallium, and gadolinium garnets", Appl. Phys. Lett., Vol. 4, pp 182-184, 1964.
- 7) R. A. Fields, M. Birnbaum, and C. L. Fincher, "Highly Efficient Nd:YOV₄ Diode-Laser End-Pumped Laser", Applied Phys. Lett., 51, pp. 1885-1886, 1987.
- 8) T. S. Lomheim, L. G. DeShazer, "Optical Absorption Intensities of Trivalent Neodymium in the Uniaxial Crystal Yttrium Orthovanadate", J. Appl. Phys., 49, pp. 5517-5522, 1976.
- 9) A.L. Harmer, A. Linz, and D.R. Gabbe, "Fluorescence of Nd³⁺ in lithium yttrium fluoride", J. Phys. Chem. Sol., Vol. 30, pp 1483-1487, 1969.

- 10) D. Pruss, G. Huber, and A. Beimososki, "Efficient Cr^{3+} sensitized $\text{Nd}^{3+}:\text{GdScGa}$ -garnet laser at $1.06 \mu\text{m}$ ", Appl. Phys. B., Vol. 28, pp 355-358, 1982.
- 11) B. I. Denker, A. A. Izyneev, I. I. Kuratec, Yu. V. Tsvetkov, and A. V. Shestakov, "Lasing in Phosphate Glasses with High Neodymium Ion Concentrations Under Pumping with Light-Emitting Diodes", Sov. J. QE, 10, pp. 1167-1168, 1980.
- 12) H. P. Jenssen, R. F. Begley, R. Webb, R. C. Morris, "Spectroscopic properties and laser performance of Nd^{3+} in lanthanum beryllate", J. Appl. Phys, 47, pp. 1496-1500, 1976.
- 13) D.L. Dexter, "A Theory of Sensitized Luminescence on Solids", J. of Chemical Physics, Vol. 21, No. 5, May 1953, pp 836-850.
- 14) C. B. Bair and P. L. Cross, "Wideband Birefringent Filter Design", submitted to Optics Letters.
- 15) J. C. Barnes, N. P. Barnes, and G. E. Miller, "Master Oscillator Power Amplifier Performance of $\text{Ti}:\text{Al}_2\text{O}_3$ ", IEEE J. of Quant. Elect., QE 24, 1988.
- 16) H. Kogelnik and T. Li, "Laser Beams and Resonators", Applied Optics, Vol. 5, No. 10, pp 1550-1566, 1966.
- 17) J. C. Barnes, N. P. Barnes, G. E. Lockard, and P. L. Cross, "Amplified Spontaneous Emission Measurement of a Line Narrowed, Tunable $\text{Ti}:\text{Al}_2\text{O}_3$ Amplifier Using Rubidium Absorption", Tunable Solid State Laser Conference, Cape Cod, Massachusetts, 1989.
- 18) U. O. Farrukh, A. M. Bouncristiani, and C. E. Byvik, "An Analysis of the Temperature Distribution in Finite Solid-State Laser Rods", J. of Quantum Electronics, Vol. 24, No. 11, pp 2253-2263, November 1988.

Table 1: SUMMARY OF EXISTING LASER MODELING SOFTWARE

Efficiency calculations

- Flashlamp pumped laser absorption efficiency
- Laser diode pumped laser absorption efficiency
- User supplied spectra pumped laser absorption efficiency
- Radial distribution of absorbed energy
- Sensitizer transfer rate calculated from Dexter integrals

Electro-optical components

- Birefringent filter
- Fabry-Perot etalon
- Nonlinear elements

Laser Amplifier and resonator models

- Pulse amplifier model
- Laser resonator - Gaussian ray trace model

Miscellaneous models

- Rb cell transmission
- Temperature distribution in the laser rod

Table 2: SAMPLE ABSORPTION SPECTRA HEADER

```

11100 15 1 01NYAG8.SP PNYAG8 MS .0000 U S1 012288 00.01 1
PROGRAM PE-CONVERT VER 02.30
USER MS DATE & TIME 1988 01 28 14.56 53.08 1.8000 295K U
AU1 ND 100 0 0 YAG 0.500000 - 0.830000 . 00010
FILE NAME ON PE-3600 = 001 NYAG8.SP ON PC = 001NYAG8.SP
NO_POINTS = 3301. pts DATA_INTV = 0.000100  $\mu$ m
MIN_LAMBDA = 0.500000  $\mu$ m MIN_DATA = 0.
MAX_LAMBDA = 0.830000  $\mu$ m MAX_DATA = 159180.
SCANSPEED = .015  $\mu$ m/min SLITWIDTH = 0.00020  $\mu$ ITA = 0.
RESP = 0.5 sec ISMS = 0. DATE = 88/01/22
INST = 509. ? = 0.
THIS IS A ND:YAG SAMPLE FOUND IN CHUCKS LAB. ASSUMED 1% CONCENTRATION. SAMPLE
1.8 MM THICK. STORM
CHANGED TO AU BY MARK STORM ON 3/4/88. HEADER DONE BY HAND.
ND:YAG,1%ND,1.8MM,HIGH RES FINAL SCAN, STORM
EOH (1X,F11.4)
3301.
1429.9563 = DATA VALUE AT 0.500000  $\mu$ m
1437.0537
1372.1863
1262.9418
1348.7021
1140.5082
1260.2499
1246.8193

```

Table 3: HEADER INFORMATION COMMON TO ALL FILES

```

Data file code
Number of lines of file header to be appended to output file
header
Number of columns in the data section of the file
Filename when the file was created
Name, major version number, and minor version number of the
program which created the file
User's initials
Data and time the file was created
One line comment entered by the user at run time
Comments, programmed by software developer
Comments contain any notes which the program developer deem appropriate and
usually include but are not limited to column labels, format of the data
section, echo of the input data. The comments section is, hopefully,
detailed enough to allow the user to associate output data with a
particular set of input data.
Appropriate lines from input file header
End-of-Header record
Number of data points in the data section

```

Table 4: HEADER INFORMATION UNIQUE TO SPECTRA HEADERS

Type of data
 Ab = Absorption
 Tm = Transmission
 Au = Absorption for unity concentration
 Em = Emission
 En = Normalized emission
 Correction flag (0 = raw data, 1 = corrected data)
 Active atom name and concentration, host
 Sensitizers 1 & 2 names and concentrations
 Minimum and maximum wavelength, resolution in micrometers
 Sample thickness in meters
 Measurement temperature in Kelvin
 Sample Polarization/ Direction of Propagation, # if inappropriate
 Recording machine (Perkin-Elmer, Spex, etc.)
 Operator's name or initials
 Excitation wavelength (emission measurements only)
 Excitation (source) polarization, # if inappropriate
 Detector type
 Date measurement was taken
 Comments, added by the spectroscopist during file transfer
 Comments include any information which the spectroscopist deems to be appropriate. Examples of appropriate information include, but are not limited to the following:
 Growth technique
 Age of sample and previous history, if appropriate (i.e., used sample for 6 months in a laser before measuring the spectra)
 Quality of the sample (good, cloudy, possibly contaminated, rough surface polish, etc.)
 Sample manufacturer / division / individual
 Institution/ division/ individual measuring spectra, if measured outside of LaRC

SOFTWARE SYSTEM FOR LASER DESIGN

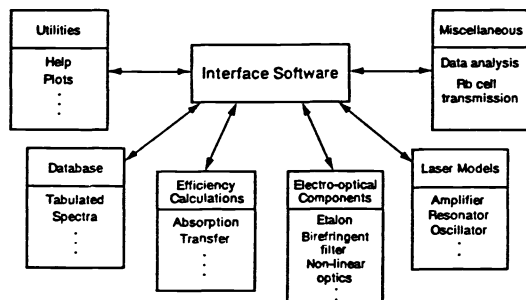


Figure 1. Schematic representation of the major elements of the software system for laser design.

DIRECTORY STRUCTURE FOR THE SYSTEM FOR LASER DESIGN

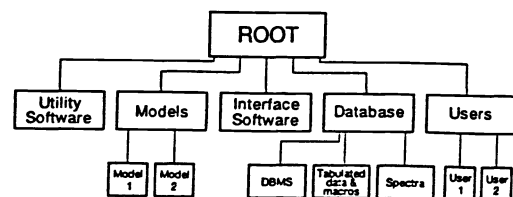


Figure 2. Schematic representation of the directory structure for the software system for laser design.

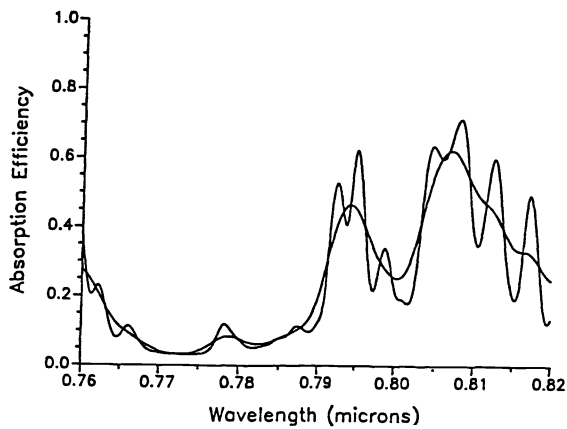


Figure 3. Absorption efficiency as a function of wavelength for a laser diode pumped Nd:YAG rod laser. The laser rod is 2.0 mm radius with 1% atomic Nd concentration. The two curves represent two laser diode center wavelengths of FWHM .001 micrometers and .004 micrometers.

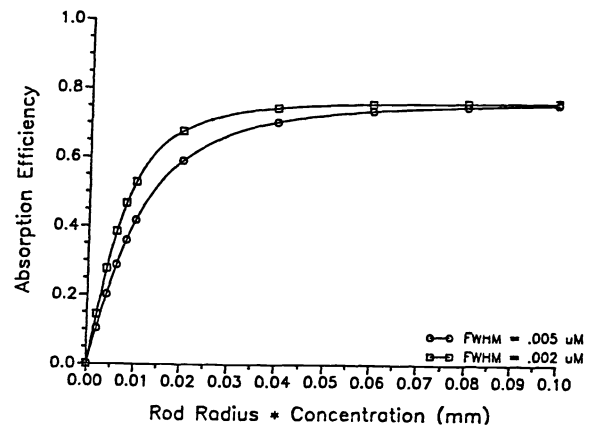


Figure 4. Absorption efficiency as a function of rod size X concentration for a laser diode pumped Nd laser. The laser diode center wavelength is .808 micrometers.

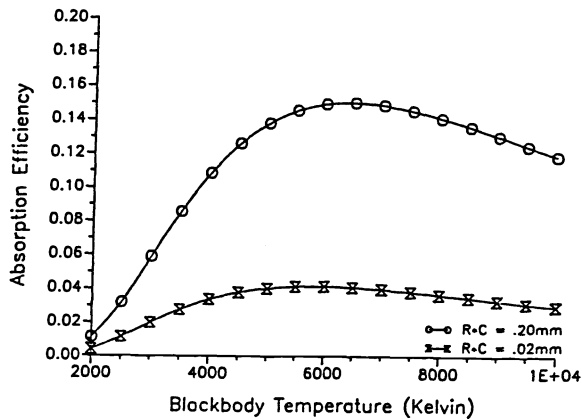


Figure 5. Absorption efficiency as a function of blackbody temperature for a Nd-doped rod laser.

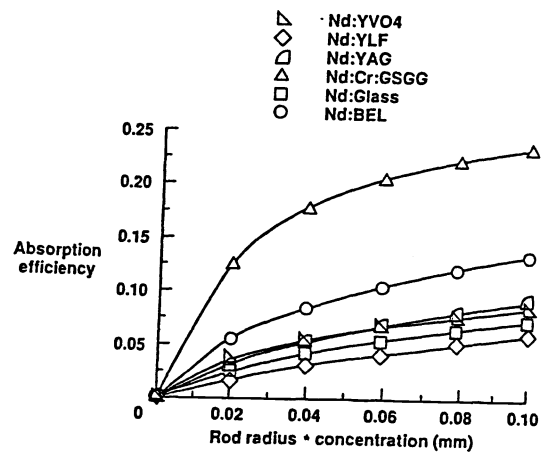


Figure 6. Absorption efficiency as a function of rod size X dopant concentration for six Nd-doped laser materials.

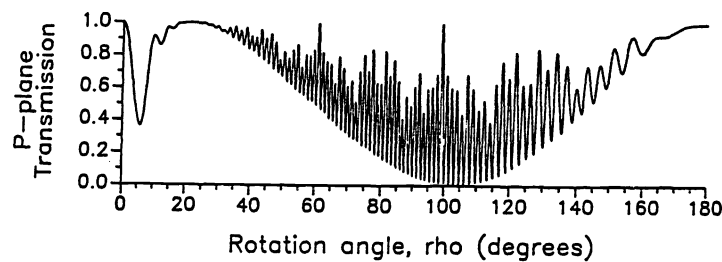


Figure 7. P-Plane transmission as a function of rotation angle for a birefringent filter.

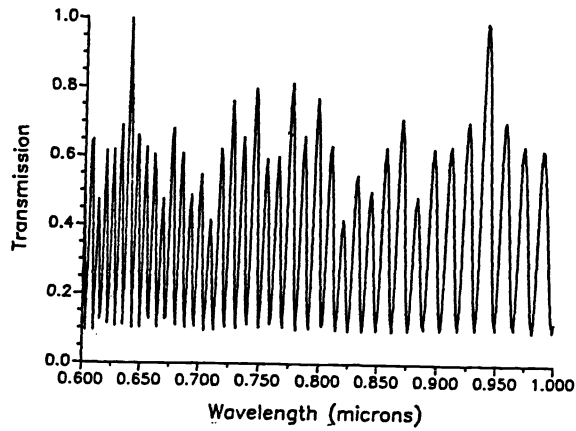


Figure 8. P-Plane transmission as a function of wavelength for a birefringent filter.

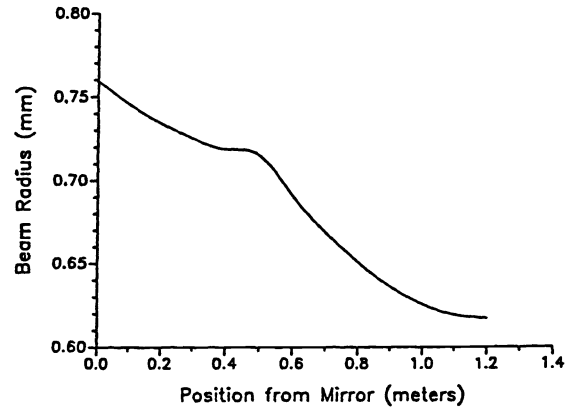


Figure 9. Beam size as a function of distance from the input mirror for a 3-element laser resonator.